Self-Assembly and Lipid Interactions of Diacylglycerol Lactone Derivatives Studied at the Air/Water Interface

Liron Philosof-Mazor,[†] Roman Volinsky,[†] Maria J. Comin,[‡] Nancy E. Lewin,[§] Noemi Kedei,[§] Peter M. Blumberg,[§] Victor E. Marquez,*[,‡] and Raz Jelinek*[,†]

Department of Chemistry and Ilse Katz Institute for Nanotechnology, Ben Gurion University, Beer Sheva 84105, Israel;, Laboratory of Medicinal Chemistry, Center for Cancer Research, National Cancer Institute at Frederick, National Institutes of Health, Frederick, Maryland 21702, Laboratory of Cancer Biology and Genetics, Center for Cancer Research, National Cancer Institute, National Institutes of Health, Bethesda, Maryland 20892

Received May 29, 2008. Revised Manuscript Received July 13, 2008

Synthetic diacylglycerol lactones (DAG-lactones) have been shown to be effective modulators of critical cellular signaling pathways. The biological activity of these amphiphilic molecules depends in part upon their lipid interactions within the cellular plasma membrane. This study explores the thermodynamic and structural features of DAG-lactone derivatives and their lipid interactions at the air/water interface. Surface-pressure/area isotherms and Brewster angle microscopy revealed the significance of specific side-groups attached to the terminus of a very rigid 4-(2-phenylethynyl)benzoyl chain of the DAG-lactones, which affected both the self-assembly of the molecules and their interactions with phospholipids. The experimental data highlight the formation of different phases within mixed DAG-lactone/phospholipid monolayers and underscore the relationship between the two components in binary mixtures of different mole ratios. Importantly, the results suggest that DAG-lactones are predominantly incorporated within fluid phospholipid phases rather than in the condensed phases that form, for example, by cholesterol. Moreover, the size and charge of the phospholipid headgroups do not seem to affect DAG-lactone interactions with lipids.

Introduction

Lipophilic second messenger *sn*-1,2-diacylglycerol (DAG) is a prominent factor in numerous signal transduction pathways associated with the onset of cancer.[1,2] Enzymes from the protein kinase C (PKC) family in particular have been identified as central mediators in DAG signaling and as attractive targets for cancer chemotherapy.[3] In recent years, the Marquez laboratory has been intensively exploring pharmacophore-guided approaches to the synthesis of conformationally restricted DAGs as potent modulators of PKC.[4] Libraries of DAG-lactones exhibiting different functional moieties have been constructed, and members of such libraries were shown to effectively translocate PKC to membranes and induce a number of downstream events such as apoptosis, AP-1 activation, and cell proliferation inhibition.[5]

Previous results obtained with DAG-lactones containing acyl chains with an ensemble of repetitive oligo(*p*-phenyleneethynylene) units that form a rigid rod showed that the ideal length of the rod consisted of two units as represented by compound **3** (Table 1).[6] Because the end residue of the rod is believed to interact with the inner layer of the membrane and could modulate its surrounding environment, we have focused on a group of compounds in which the acetylene terminus of **3** has been replaced with other residues, including hydrogen, methoxy, or phenyl, designed to explore the roles of R residues of different sizes and electronic properties (Table 1).

Table 1. DAG-lactone Structures Examined, log *P* Values,[7] and Binding Affinities (K_i) for PKC-α

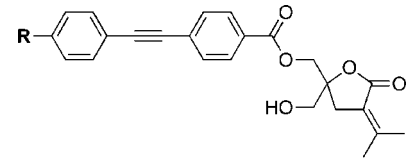

compound	R	log *P*	K_i (nM)
1	H	3.26	6.6 ± 0.6
2	OCH_3	3.27	7.1 ± 1.1
3	C≡C	3.24	6.0 ± 1.1
4	Ph	4.92	6.4 ± 1.1

The compounds depicted in Table 1 showed similar binding potencies for recombinant PKC-α, assayed by competition for binding with [20-^{3}H]phorbol 12,13-dibutyrate in the presence of 100 μg/mL phosphatidylserine (Table 1). It is recognized, however, that the phospholipids represent a half-site for the ligand binding along with the C1 domains of the PKC, and these assay conditions are optimized for the contribution of the lipids.[4−6]

* To whom correspondence should be addressed. (V.E.M.) E-mail: marquezv@mail.nih.gov. (R.J.) E-mail: razj@bgu.ac.il.

† Ben Gurion University.

‡ Laboratory of Medicinal Chemistry, National Institutes of Health.

§ Laboratory of Cancer Biology and Genetics, National Institutes of Health.

(1) Griner, E. M.; Kazanietz, M. G. *Nat. Rev. Cancer* **2007**, *7*, 281294. Protein kinase C and other diacylglycerol effectors in cancer.

(2) Nishizuka, Y. *Science* **1992**, *258*, 607614. Intracellular signaling by hydrolysis of phospholipids and activation of protein-kinase-C.

(3) Mackay, H. J.; Twelves, C. J.; *Nat. Rev. Cancer* 2007, *7*, 554–562. Targeting the protein kinase C family: are we there yet.

(4) Marquez, V. E.; Blumberg, P. M.; *Acc. Chem. Res.* 2003, *36*, 434–443. Synthetic diacylglycerols (DAG) and DAG-lactones as activators of protein kinase C (PK-C).

(5) Pu, Y.; Perry, N. A.; Yang, D.; Lewin, N. E.; Kedei, N.; Braun, D. C.; Choi, S. H.; Blumberg, P. M.; Garfield, S. H.; Stone, J. C.; Duan, D.; Marquez, V. E.; *J. Biol. Chem.* 2005, *280*, 27329–27338. A novel diacylglycerol-lactone shows marked selectivity in vitro among C1 domains of protein kinase C (PKC) isoforms alpha and delta as well as selectivity for RasGRP compared with PKC alpha.

(6) Malolanarasimhan, K.; Kedei, N.; Sigano, D. M.; Kelley, J. A.; Lai, C. C.; Lewin, N. E.; Surawski, R. J.; Pavlyukovets, V. A.; Garfield, S. H.; Wincovitch, S.; Blumberg, P. M.; Marquez, V. E.; *J. Med. Chem.* 2007, *50*, 962–978. Conformationally constrained analogues of diacylglycerol (DAG). 27. Modulation of membrane translocation of protein kinase C (PKC) isozymes alpha and delta by diacylglycerol lactones (DAG-lactones) containing rigid-rod acyl groups.

(7) Wildman, S. A.; Crippen, G. M.; *J. Chem. Inf. Comput. Sci.* 1999, *39*, 868–873. Prediction of physicochemical parameters by atomic contributions.

10.1021/la802204n CCC: $40.75
Published on Web 09/13/2008

Under physiological conditions, in contrast, the specific lipid environment will be colimiting along with the ligand, and differences in ligand − phospholipid interactions would thus be expected to affect the formation of complexes with other signaling or scaffolding proteins that facilitate signal transduction and confer specificity for individual PKC isoforms by regulating their activity and cellular localization.[8−10] Furthermore, these signaling complexes are not confined to the plasma membrane alone but are also found on various cellular membranes, including Golgi, mitochondrial, and nuclear membranes, all of which have different lipid compositions.[11,12] Therefore, it is not surprising that the specific nature of the side chains on the phorbol or DAG-lactone templates has been found to make a major contribution to their selectivity of action.[4−6]

This study seeks to characterize the interactions between the side chains of DAG-lactones and constituents of physiological membranes, viz., phospholipids and cholesterol. The thrust of this work is that a better understanding of lipid interactions will guide efforts at ligand design to exploit variations in membrane composition, whether between different membrane compartments within the same cell or differences *between* cell types.

Numerous studies have analyzed the self-assembly and molecular organization at the air/water interface (i.e., Langmuir trough). In particular, Langmuir monolayers constitute an effective vehicle for studying self-assembly properties of amphiphilic molecules and their lipid interactions and membrane association.[13−15] Langmuir monolayers have been particularly informative as models for studying organization and membrane interactions of membrane-active peptides and other amphiphilic biomolecules. The preferred localization of amphiphilic biological molecules at the water surface and the presence of a defined interface constitute an environment in which membrane-active molecules can self-assemble.[13−15]

Particularly important in the context of studying membrane interactions of biological molecules has been the deposition of phospholipid monolayers at the air/water interface.[13] Phospholipid monolayers have been employed in various investigations of peptide−membrane interactions, yielding information both on the cooperative properties of lipid-interacting peptides and on the organization and disruption of the lipid layers following interactions of amphiphilic species.[13,14] In most instances, physical and morphological analyses of Langmuir film/peptide assemblies have been conducted by thermodynamic methods (pressure−area isotherms) and microscopy techniques (fluorescence microscopy and Brewster angle microscopy).[19] Here we present a thermodynamic and Brewster angle microscopy analysis of DAG-lactone properties at the air/water interface and their interactions with lipid monolayers. The experiments reveal significant differences in self-assembly properties of the compounds and the effects of the R residues upon lipid interactions.

Materials and Methods

Synthesis. Detailed description of the synthetic routes and product characterization are found in the Supporting Information. Briefly, the core lactone (5,5-bis(hydroxymethyl)-3-(methylethylidene)-γ-butyrolactone)[6] was monoprotected with the *p*-methoxyphenyl (PMP) group and acylated at the *sn*-1 position with a series of polyaromatic carboxylic acids with different terminal **R** groups. The carboxylic acids were prepared by Sonogashira coupling[16] of 1,1-dimethyl-1-silaethyl 4-ethynylbenzoate with the corresponding *p*-substituted aryl iodides, similar to the preparation of **3**.[6] After cleavage of the trimethylsilylethanol protecting group, the carboxylic acids were obtained in crystalline form and used without further purification for the coupling reaction with the protected lactone. The coupling was performed by reacting the carboxylic acids with the lactone in the presence of BOPCl and DMAP.[17] All final products were obtained in good yields after final deprotection of the PMP group (Scheme 1).

Materials. 1,2-Dimyristoyl-*sn*-glycero-3-phosphocholine (DMPC), 1,2-dimyristoyl-sn-glycero-3-phosphoglycerol (DMPG), and cholesterol were purchased from Avanti Polar Lipids (Alabaster, AL). Chloroform ($CHCl_3$) was HPLC grade (Frutarom Ltd.).

Parent solutions of the phospholipids and DAG-lactones were prepared by dissolution in chloroform to a concentration of 2 mM. The various mole fractions were prepared by mixing the appropriate amounts of parent solutions of each compound.

The water subphase used in the Langmuir trough was doubly purified with a Barnstead D7382 water purification system (Barnstead Thermolyne Corporation, Dubuque, IA), yielding 18.3 mΩ resistivity.

Analysis of Inhibition of [^{3}H]PDBu Binding by Ligands 1−4 Enzyme−ligand interactions were analyzed by competition with [^{3}H]PDBu binding to the single isozyme PKC-α essentially as described previously.[18] The ID_{50} values were determined by least-squares fitting of the theoretical sigmoidal competition curve to the binding data. The K_i values were calculated from the ID_{50} values according to the relationship $K_i = ID_{50}/(1 + L/K_d)$, where L is the concentration of free [^{3}H]PDBu at the ID_{50} and K_d is the dissociation constant for [^{3}H]PDBu under the assay conditions.

Values represent the mean ± standard error (three determinations). The octanol/water partition coefficients (log *P*) were calculated according to the atom-based program MOE Slog *P*.[7]

Translocation of GFP-Tagged PKC Isoforms in CHO Cells. CHO cells were purchased from the American Type Culture Collection (Manassas, VA) and cultured in F12-K medium supplemented with 10% fetal bovine serum and antibiotics (50 units/mL penicillin and 0.05 mg/mL streptomycin). CHO cells plated onto T delta dishes (Bioptechs Inc., Butler, PA) were transfected with GFP-tagged PKC-α or PKC-δ using Lipofectamine reagent (Invitrogen, Carlsbad, CA). For confocal images, cells were examined with a Zeiss LSM 510 confocal microscope (Carl Zeiss Inc., Thornwood, NY) with an Axiovert 100 M inverted microscope operating with a 25 mW argon laser tuned to 488 nm. Cells were imaged with a 63 × 1.4 NA Zeiss Plan-Apochromat oil-immersion objective and with varying zooms (1.4 to 2). Time-lapse images were collected every 30 s using Zeiss AIM software in which the green emission was collected in a PMT with an LP 505 filter.

Surface-Pressure/Area Isotherms. All surface-pressure/area isotherms were recorded using a computerized Langmuir trough (model 622/D1, Nima Technology Ltd., Coventry, U.K.). The surface pressure was monitored using 1-cm-wide filter paper as a Wilhelmy

(8) Poole, A. W.; Pula, G.; Hers, I.; Crosby, D.; Jones, M. L.; *Trends Pharmacol. Sci.* 2004, *25*, 528–535.PKC-interacting proteins: from function to pharmacology.
(9) Schechtman, D.; Mochly-Rosen, D.; *Oncogene* 2001, *20*, 6339–6347. Adaptor proteins in protein kinase C-mediated signal transduction.
(10) Teicher, B. A.; *Clin. Cancer Res.* 2006, *12*, 5336–5345. Protein kinase C as a therapeutic target.
(11) Neri, L. M.; Borgatti, P.; Capitani, S.; Martelli, A. M.; *Histol. Histopath.* 2002, *17*, 1311–1316. Protein kinase C isoforms and lipid second messengers: a critical nuclear partnership.
(12) Wong, W.; Scott, J. D.; *Nat. Rev. Mol. Cell Biol.* 2004, *5*, 959–970. AKAP signalling complexes: Focal points in space and time.
(13) Fidelio, G. D.; Maggio, B.; Cumar, F. A.; *Biochim. Biophys. Acta* 1986, *862*, 49–56. Interaction of melittin with glycosphingolipids and phospholipids in mixed monolayers at different temperatures. Effect of the lipid physical state.
(14) Maget-Dana, R.; *Biochem. Biophys. Acta* 1999, *1462*, 109–140. The monolayer technique: a potent tool for studying the interfacial properties of antimicrobial and membrane-lytic peptides and their interactions with lipid membranes.
(15) Thomas, C. J.; Surolia, N.; Surolia, A.; *J. Biol. Chem. Biol.* 2001, *276*, 35701–35706. Kinetic and thermodynamic analysis of the interactions of 23-residue peptides with endotoxin.
(16) Chinchilla, R.; Nájera, C.; *Chem. Rev.* 2007, *107*, 874–922.The Sonogashirar reaction: A booming methodology in synthetic organic chemistry.
(17) Diago-Meseguer, J.; Palomo-Coll, A.; *Synthesis* 1980, 547–551. A new reagent for activating carboxyl groups; preparation and reactions of N,N-bis[2-oxo-3-ox-azolidinyl]phosphorodiamidic chloride.
(18) Lewin, N. E.; Blumberg, P. M. *Methods Mol. Biol.* **2003**, *233*, 129–156. [3H]-Phorbol 12,13-dibutyrate binding assay for protein kinase C and related proteins.

Scheme 1. Syntheses of DAG-lactones (Table 1)[a]

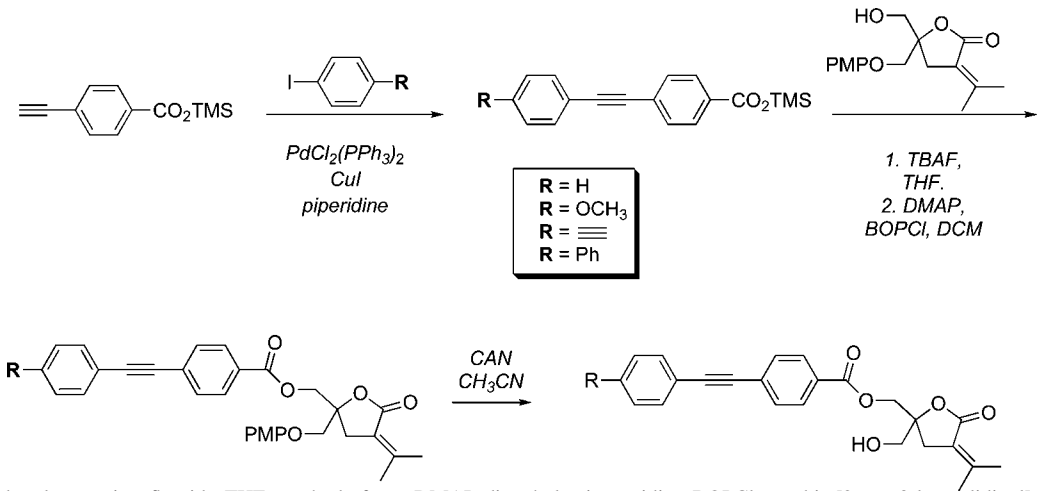

[a] TBAF, *n*-tetrabutylammonium fluoride; THF, tetrahydrofuran; DMAP, dimethylaminopyridine; BOPCl, *N*,*N*-bis-[2-oxo-3-lx-azolidinyl]phosphorodiamidic chloride; DMC, dichloromethane; CAN, ceric ammonium nitrate.

plate. For each isotherm experiment, the desired amount of DAG-lactone or lipid/DAG-lactone mixture in chloroform (total concentration of 2 mM) was spread on the water subphase and equilibrated for 15 min, allowing for solvent evaporation prior to compression. Compression was carried out at a constant barrier speed of 8 cm^2 min^{-1}. Each isotherm represents three experimental runs, which were reproducible within an error of 1.0 $Å^2$ $molecule^{-1}$.

Brewster Angle Microscopy (BAM). The Brewster angle microscope (NFT, Gottingen, Germany) mounted on a Langmuir film balance was used to observe the microscopic structures in situ. The light source of the BAM was a frequency-doubled Nd:YAG laser with a wavelength of 532 nm and 20−70 mW primary output power in a collimated beam. The BAM images were recorded with a CCD camera. The scanner objective was a Nikon superlong working distance objective with nominal 10× magnification and a diffraction-limited lateral resolution of 2 μm. The images were corrected to eliminate side ratio distortion originating from a nonperpendicular line of vision of the microscope.

Results

Table 1 depicts the chemical structures of the DAG-lactone derivatives examined in this work, which incorporate a rigid 4-[2-(R-phenyl)ethynyl]benzoate moiety in the acyl position.[6] Because these highly conjugated systems tend to form molecular aggregates and incorporate within membrane bilayers, the air/water experiments were designed to explore the effect on molecular aggregation and lipid interactions of changing the chemical nature of the terminal R group at the end of the chain of the most important prototype (compound **3**) that was discovered earlier.[7] In particular, we aimed to probe whether the shape-persistent architecture of DAG-lactones **1**−**4** would induce important changes in organization and lipid interactions.

Membrane Translocation Analysis. Figure 1 depicts representative confocal microscopy images of CHO cells overexpressing GFP-PKC isozymes α and δ following treatment with **1**. The kinetic profile apparent in Figure 1 points to a dramatic difference in the translocation of each isozyme to distinct cellular compartments: PKC-α to the cell membrane and PKC-δ to internal organelles. Similar membrane targeting of PKCs α and δ albeit with different kinetics was apparent after the addition of the other DAG lactones studied (data for **3** reported in ref 6). The translocation data presented in Figure 1 highlight the critical role that the type and organization of lipids in different membranes

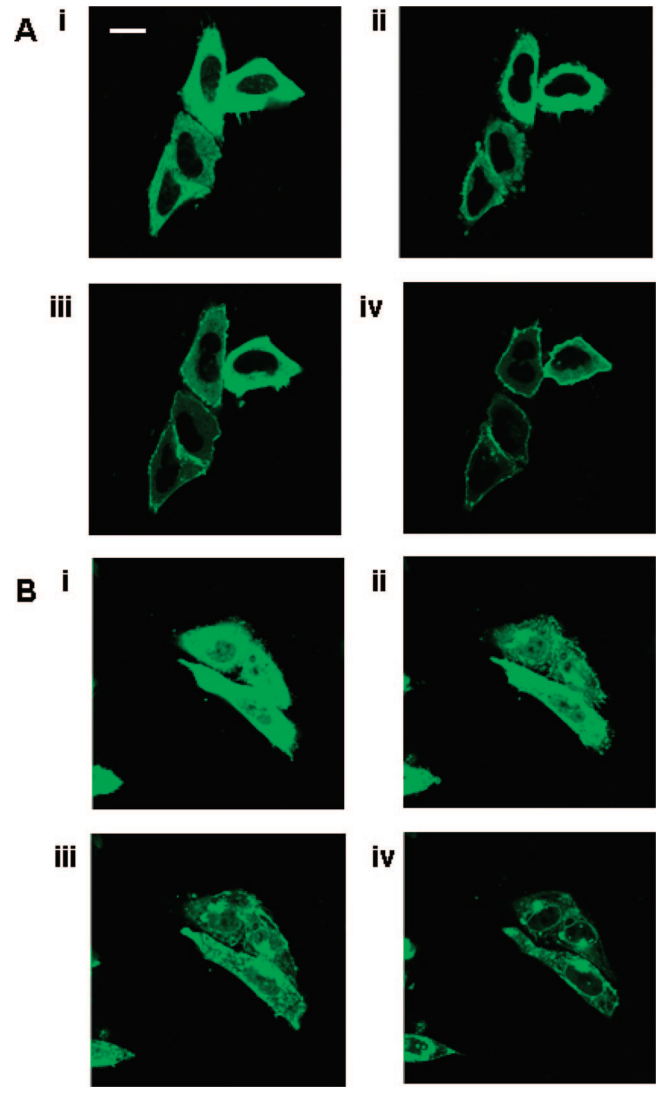

Figure 1. DAG-lactone translocation to the cellular membrane. Confocal microscopy images of CHO cells overexpressing GFP-PKC-α (A) and GFP-PKC-δ (B) following treatment with **1.** (i) 0 min after the addition of **1**; (ii) 1 min.; (iii) 10 min.; and (iv) 30 min.. The bar corresponds to 10 μm.

(19) Henon, S.; Meunier, J.; *Rev. Sci. Instrum.* 1991, *64*, 936–939. Microscope at the Brewster angle: direct observation of first-order phase transitions in monolayers.

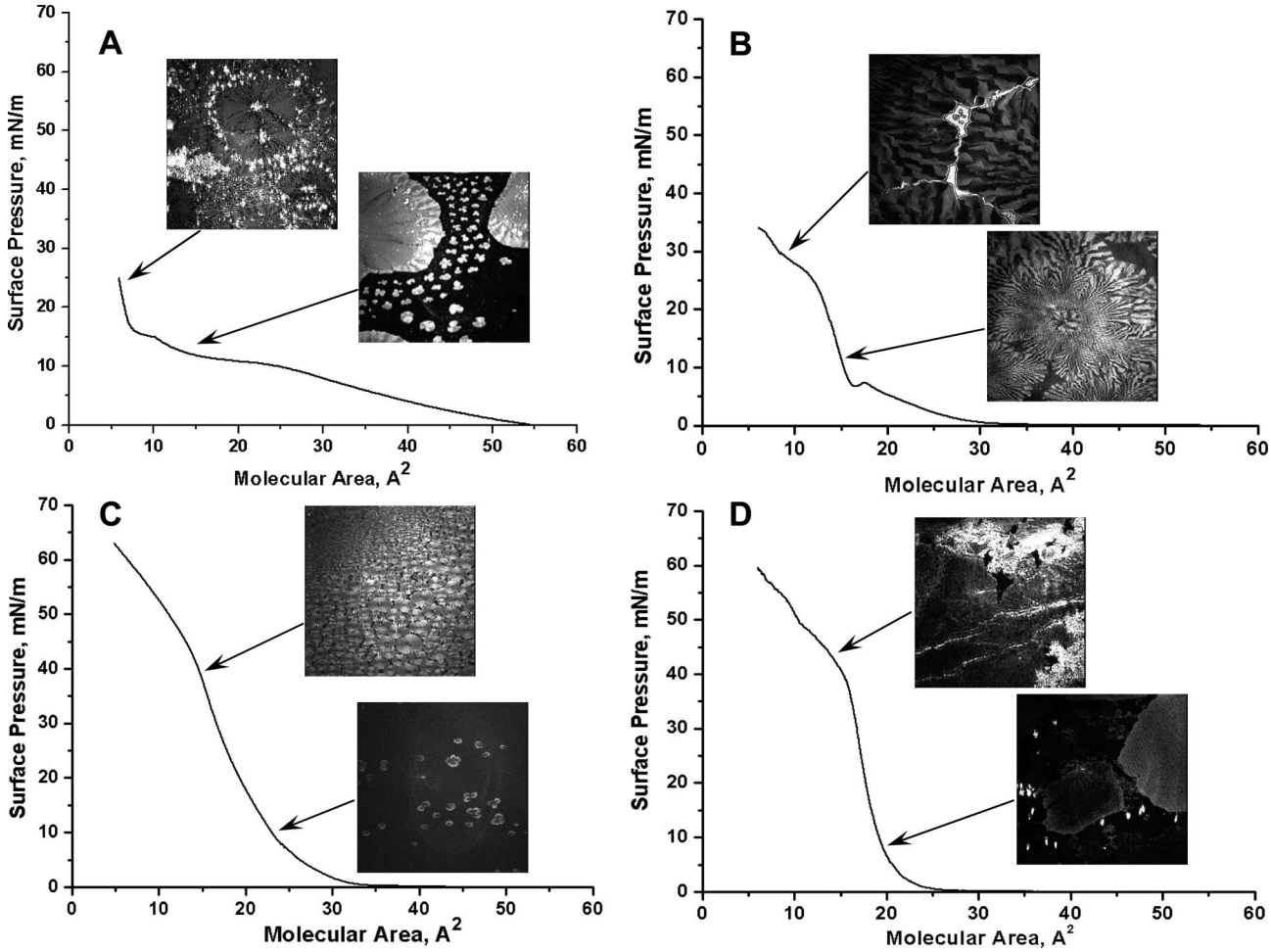

Figure 2. DAG-lactone derivatives at the air/water interface. Surface-pressure/area isotherms and BAM images recorded on a water subphase: (A) **1**, (B) **2**, (C) **3**, and (D) **4**. The BAM images were recorded at the surface pressures indicated by the arrows. The dimensions of all BAM images are 450 μm $\times$ 450 μm.

might play in directing specific molecular interactions between the DAG-lactone ligands and their biological targets.

Individual DAG-lactone Derivatives at the Air/Water Interface. Figure 2 depicts thermodynamic analyses of compounds **1**−**4** compressed at the air/water interface (surface-pressure/area (π−A) isotherms) and Brewster angle microscopy (BAM) images recorded at distinct surface pressures that were designed to probe the occurrence and configurations of condensed domains within the DAG-lactone monolayers.[19,20] The data shown in Figure 2 demonstrate that significant differences exist among the four DAG-lactones in term of their self-assembly properties.

The π−A isotherm of **1**, exhibiting hydrogen as R (Figure 2A), shows a pronounced liquid-expanded (LE) phase extending from a molecular area of around 53 Å^2 to approximately 20 Å^2. Subsequent LE−liquid condensed (LC) and LC−solid phase transitions are observed at surface pressures of 12 and 15 mN/m, respectively. The transitions lead to the formation of condensed domains of **1** that are clearly apparent in the BAM images (Figure 2A). Specifically, following the first transition at 12 mN/m, isolated round domains are formed that subsequently coalesce into a closely packed solid film past the LC−solid transition (BAM image recorded at 25 mN/m, Figure 2A). No BAM reflections were detected in the LE phase as a result of the low density of the fluid monolayer.[21]

Similar to **1**, the π−A isotherm of **2**, displaying the methoxy functional group (Figure 2B), begins with an LE phase albeit at a much smaller molecular area of approximately 35 Å^2, indicating a more compact configuration of the molecules within the fluid monolayer. The isotherm of **2** further exhibits two phase transitions at 8 and 28 mN/m ascribed to transformations into condensed phases. In particular, the first transition corresponds to coexisting expanded and condensed liquid phases,[22] exhibiting a limiting molecular area of approximately 18 Å^2. The condensed domains are apparent in the BAM image as the distinct "islands" within the dark background of the fluid phase. The second transition (around 27 mN/m) leads to film reorganization into a stable condensed phase; the appearance of the bright regions at the rims of the condensed domains of **2** further indicate the onset of monolayer collapse.[23,24]

(20) Honig, D.; Mobius, D.; *J. Phys. Chem.* 1991, *95, 12*, 4590–4592.Direct visualization of monolayers at the air-water interface by Brewster angle microscopy.

(21) Honig, D.; Overbeck, G. A.; Mobius, D.; *Adv. Mater.* 1992, *4*, 419–424. Morphology of pentadecanoic acid monolayers at the air/water interface studied by BAM

(22) Petty, M. C. *Langmuir-Blodgett Films*. Cambridge University Press: Cambridge, U.K., 1996.

(23) Siegel, S.; Honig, D.; Vollhardt, D.; Mobius, D.; *J. Phys. Chem.* 1992, *96*, 8157–8160. Direct observation of three-dimensional transformation of insoluble monolayers.

(24) Volinsky, R.; Gaboriaud, F.; Berman, A.; Jelinek, R.; *J. Phys. Chem. B* 2002, *106*, 9231–9236.Morphology and organization of phospholipid/diacetylene langmuir films studied by Brewster angle microscopy and fluorescence microscopy.

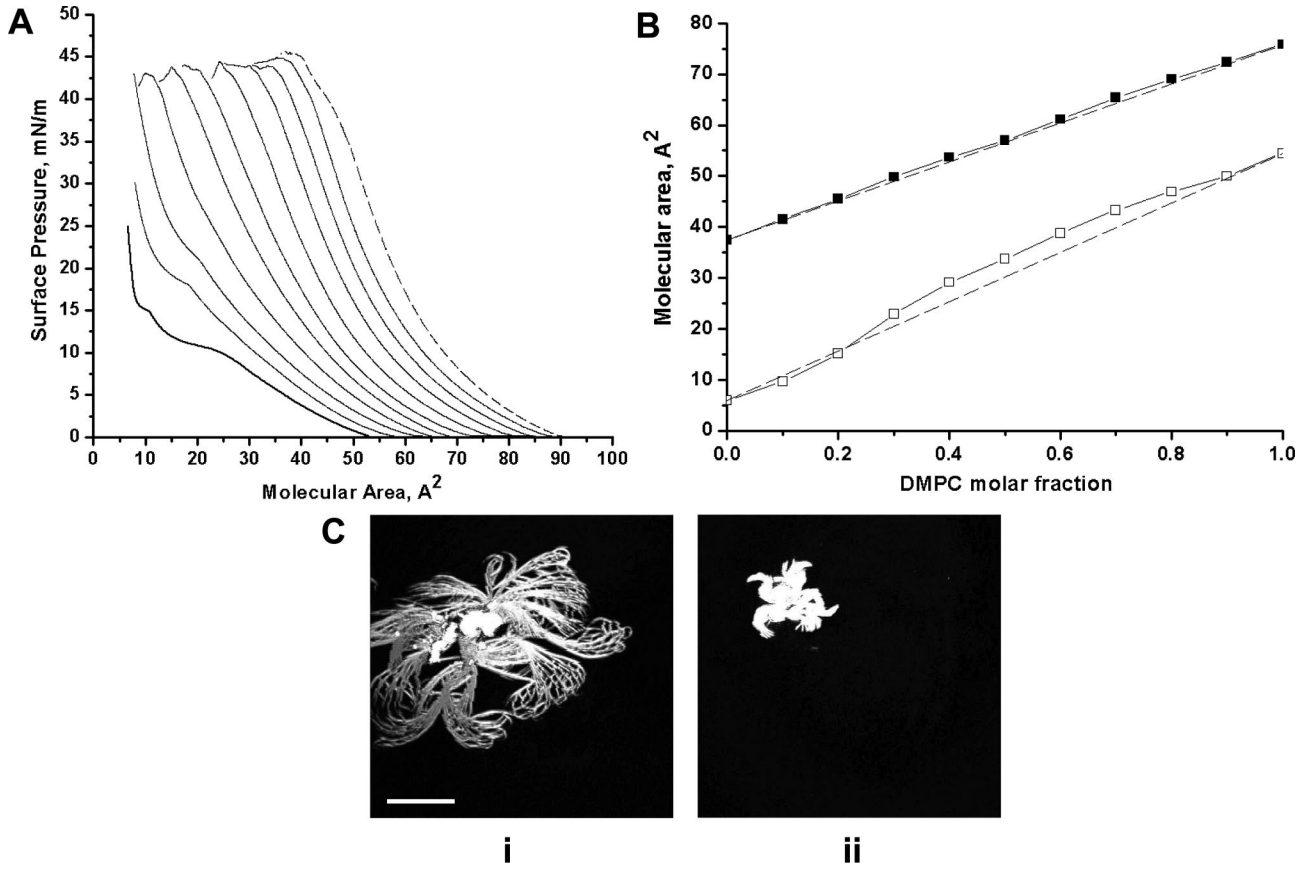

Figure 3. Mixed monolayers of **1** and DMPC. (A) $\pi-$A isotherms of monolayers having different **1**/DMPC ratios; the solid curve on the left is pure **1**, and the broken curve on the right is pure DMPC. Consecutive curves from left contain higher DMPC concentrations increasing in 10% increments (i.e., 9:1, 8:2, 7:3, etc.). (B) Additivity rule diagram; broken lines correspond to mean molecular areas predicted for ideal mixtures (noninteracting species) of **1** and DMPC. Filled squares correspond to experimental data obtained at 5 mN/m, and empty squares correspond to experimental data obtained at 25 mN/m. The height of the squares corresponds to the experimental error of the average molecular area (1 Å^2/molecule). (C) BAM images recorded at 25 mN/m for **1**/DMPC monolayers: (i) 9:1 mol ratio (**1**/DMPC) and (ii) 4:1 mol ratio. The bar corresponds to 100 μm.

The $\pi-$A isotherm and BAM data of **3** depicted in Figure 2C point to distinct differences in monolayer properties compared to those of **1** and **2**, reflecting the distinctive properties of the triple-bond residue (Table 1). Importantly, a condensed phase is formed almost immediately following the deposition and initial compression of the molecules, as exemplified in the circular domains present within the monolayer (BAM image recorded at 9 mN/m, Figure 2C). Following film collapse at 45 mN/m, the agglomeration of separate domains of **3** into a uniform film occurred (Figure 2C).

The thermodynamic profile of **4**, exhibiting the phenyl side residue, is shown in Figure 2D. The steep increase in surface pressure in the initial compression stage corresponds to a condensed phase with a limiting molecular area of 20 Å^2/molecule. Consistent with the isotherm properties, the BAM image taken at approximately 7 mN/m shows that large condensed domains were formed even at low surface pressures, covering almost the entire water surface (Figure 2D). Further compression led to monolayer collapse (transition apparent in the $\pi-$A isotherm at 40 mN/m), giving rise to the bright multilayered film apparent in the BAM image.

Mixed Monolayers of DAG-lactones and DMPC. Figures 3−6 depict the thermodynamic and BAM analyses of mixed monolayers comprising the DAG-lactone derivatives and dimyristoylphosphatidylcholine (DMPC), a saturated zwitterionic phospholipid widely used in model membrane studies.[25] The experiments summarized in Figures 3−6 were designed to examine the effect of the phospholipids on the film organization and determine to what extent the R residues influence the interactions of the DAG-lactones and the phospholipids.

Figure 3A presents the $\pi-$A isotherms of mixed monolayers of **1** and DMPC, where each isotherm was acquired for a different **1**/DMPC mole ratio. (The bold isotherm on the left corresponds to pure **1**, and the broken isotherm on the right was pure DMPC.) The compression isotherms in Figure 3A demonstrate that the LE−LC transition of **1** (observed at around 10 mN/m in pure **1**, bold isotherm in Figure 3A) appeared at increasingly higher surface pressures as the DMPC concentration in the film was increased. This result indicates that the addition of DMPC significantly stabilized the liquid-expanded phase of **1**, resulting in the occurrence of the LE−LC phase transition at higher surface pressures (Figure 3A, second and third isotherms from the left). This transition is completely eliminated at DMPC concentrations above 30% (Figure 3A, fourth isotherm from the left). Beyond this threshold, the LC−solid transition, which is apparent in the isotherm of pure **1** at 15 mN/m, disappeared. Indeed, only a liquid-expanded phase is observed when the concentration of phospholipids in the monolayer exceeds 30% (fourth to ninth isotherms from the left in Figure 3A).

(25) Tang, Z.; Jing, W.; Wang, E.; *Langmuir* 2000, *16*, 1696–1702. Self-assembled monolayer growth of phospholipids on hydrophobic surface toward mimetic biomembranes: scanning probe microscopy study.

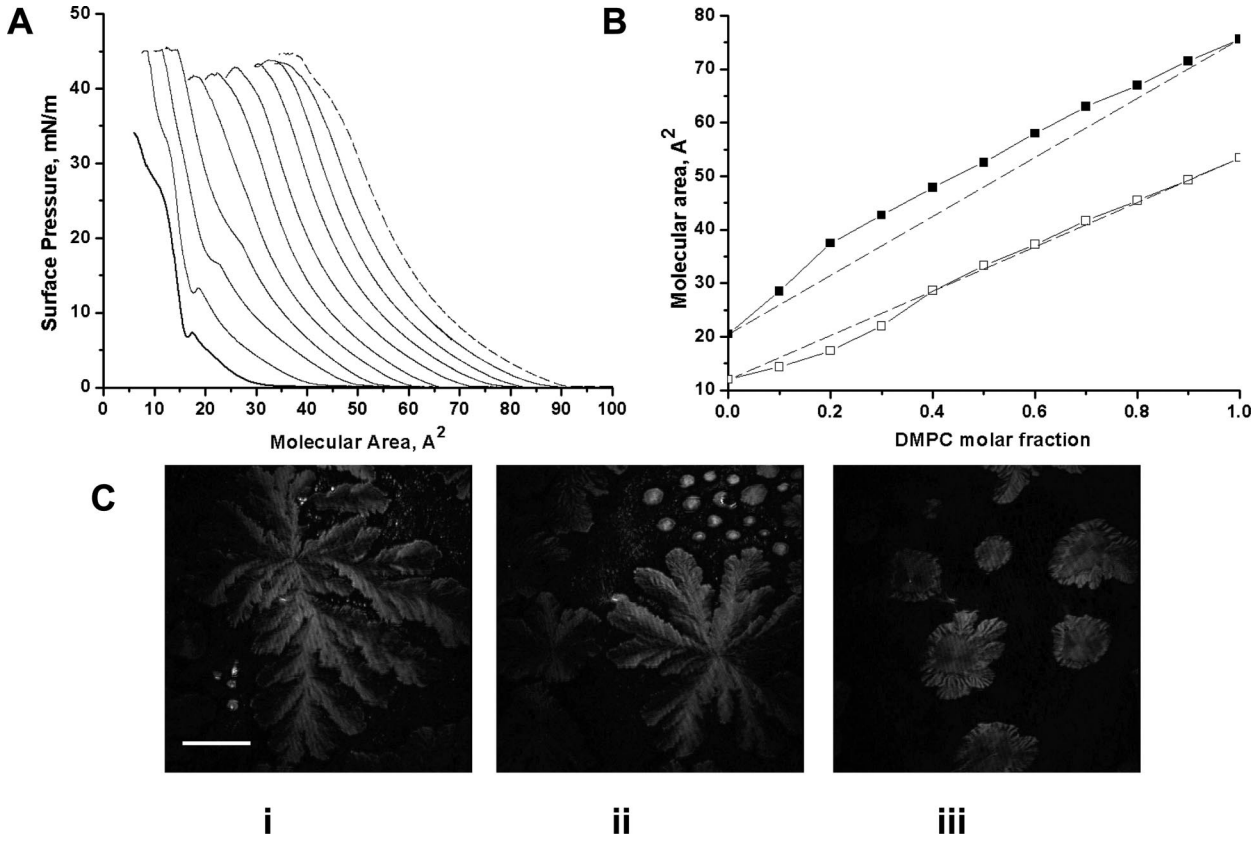

Figure 4. Mixed monolayers of **2** and DMPC. (A) $\pi-$A isotherms of monolayers having different **1**/DMPC ratios; the solid curve on the left is pure **2**, and the broken curve on the right is pure DMPC. Consecutive curves from left to right contain higher DMPC concentrations that increase in 10% increments (i.e., 9:1, 8:2, 7:3, etc.). (B) Additivity rule diagram; broken lines correspond to mean molecular areas predicted for ideal mixtures (noninteracting species) of **2** and DMPC. Filled squares represent experimental data obtained at 5 mN/m, and empty squares represent experimental data obtained at 25 mN/m. The height of the squares corresponds to the experimental error of the average molecular area (1 Å^2/molecule). (C) BAM images recorded at 20 mN/m for **2**/DMPC monolayers: (i) 9:1 mol ratio (**2**/DMPC), (ii) 4:1 mol ratio, and (iii) 7:3 mol ratio. The bar corresponds to 100 μm.

Evaluating the extent of intermolecular interactions in monolayers comprising two components is aided by the application of the additivity rule.[26] In the context of the binary monolayers of DAG-lactone and DMPC, the additivity rule predicts that in case of an ideal mixture (i.e., the two molecular components do not interact with each other) the mean molecular area (A_{mean}) at a given surface pressure will be essentially equal to the weighted average

$$A_{mean} = X_{DAG-L}A_{DAG-L} + X_{DMPC}A_{DMPC} \qquad (1)$$

where X_{DAG-L} and A_{DAG-L} are the mole fraction and molecular area of the pure DAG-lactone, respectively. X_{DMPC} and A_{DMPC} similarly correspond to the DMPC mole fraction and molecular area in a pure DMPC monolayer, respectively. Thus, a comparison of the actual experimentally obtained mean molecular areas with the values predicted by the additivity rule provides important insight into the extent of miscibility and interactions in the binary monolayer.[14,26]

Figure 3B depicts the average molecular areas in relation to the DMPC mole fractions, extracted from the isotherms in Figure 3A. The straight broken lines in Figure 3B correspond to values predicted according to the additivity rule (eq 1) (i.e., an ideal mixture). Indeed, the experimental values extracted at a low surface pressure of 5 mN/m (Figure 3B, filled squares) fall almost exactly on the straight broken line, indicating that in all mixed monolayers examined DAG-lactone **1** does not interact with DMPC. The observation of an ideal mixture at 5 mN/m is most likely ascribed to the fact that both molecules adopt a fluid liquid-expanded phase at this surface pressure, minimizing molecular interactions between them.

At 25 mN/m, however, a slight negative deviation from the straight line is detected up to an DMPC mole fraction of 0.2, followed by a positive deviation for all other binary compositions (empty squares in Figure 3B). The negative deviations (i.e., smaller molecular areas than the ones predicted from an ideal mixture) are possibly related to the different organization of the condensed DAG-lactone domains in the mixed monolayers. Indeed, the BAM images in Figure 3C that were recorded after the LE$-$LC phase transition (surface pressure of 15 mN/m) were feature domain structures that were different than the configurations observed in monolayers of pure **1** (Figure 2A). Furthermore, the condensed regions were observed only in mixed monolayers containing at least 80% **1**. This result is consistent with the isothermal analyses in Figure 2A,B, indicating that monolayers in which the DMPC mole ratio exceeds 0.3 comprise a single fluid phase in which the two components are completely miscible.

Figure 4 depicts the thermodynamic and BAM analysis of **2**/DMPC monolayers. The isotherms recorded for the **2**/DMPC mixtures (Figure 4A) point to the formation of a dominant LE phase when higher phospholipid concentrations are incorporated into the DAG-lactone monolayer, resulting in a progressive increase in the LE$-$LC transition pressure. Specifically, the transition occurring at 7 mN/m in pure **2** (bold isotherm in Figure 4A) shifted to approximately 13 mN/m in the monolayer containing 10% DMPC (second isotherm from left in Figure 4A) and to approximately 17 mN/m for 20% DMPC (third isotherm

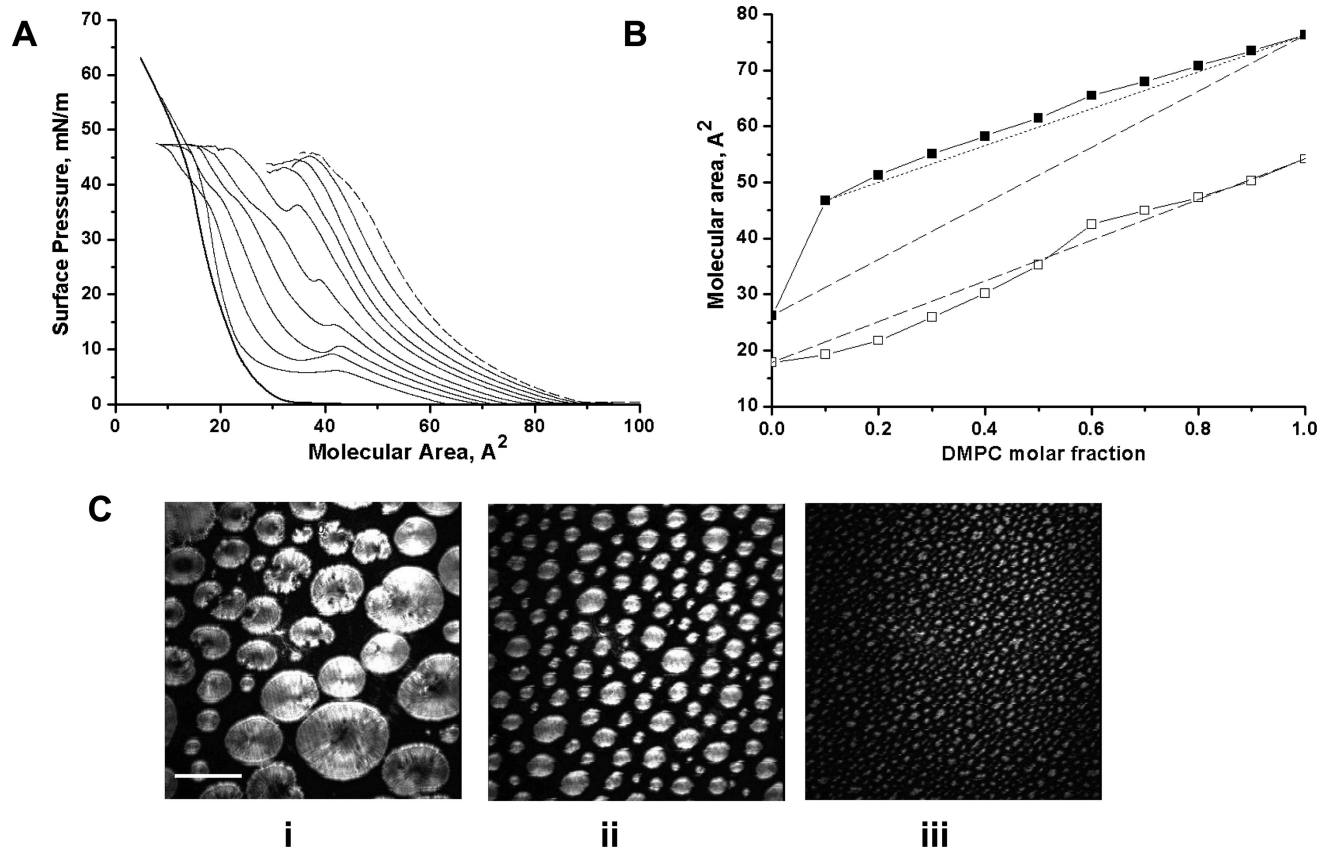

Figure 5. Mixed monolayers of **3** and DMPC. (A) $\pi-$A isotherms of monolayers having different **1**/DMPC ratios; the solid curve on the left is pure **3**, and the broken curve on the right is pure DMPC. Consecutive curves from left to right contain higher DMPC concentrations that increase in 10% increments (i.e., 9:1, 8:2, 7:3, etc.). (B) Additivity rule diagram; broken lines correspond to mean molecular areas predicted for ideal mixtures (noninteracting species) of **3** and DMPC. Filled squares represent experimental data obtained at 5 mN/m (the dotted straight line traces the points at which the mixed **3**/DMPC monolayer adopted an LE phase; see the text), and empty squares represent the experimental data obtained at 25 mN/m. The height of the squares corresponds to the experimental error of the average molecular area (1 Å^2/molecule). (C) BAM images recorded at 15 mN/m for **3**/DMPC monolayers: (i) 9:1 mol ratio (**3**/DMPC), (ii) 4:1 mol ratio, and (iii) 7:3 mol ratio. The bar corresponds to 100 μm.

from left). Indeed, similar to the mixed monolayers of **1** and DMPC described above (Figure 3A), the **2**/DMPC monolayers turn completely LE beyond a DMPC mole ratio threshold of 0.4 (fifth isotherm from left in Figure 4A).

The additivity rule analysis in Figure 4B, however, reveals significant differences between lipid interactions of **2** and **1**. In particular, whereas at a low surface pressure of 5 mN/m the **1**/DMPC monolayers looked like ideal mixtures (thus yielding mean molecular areas predicted by the additivity rule, filled squares in Figure 3B), the monolayers of **2** and DMPC at the same surface pressure exhibited significant positive deviation at all mole fractions (Figure 4B, filled squares). Differences in **2**/DMPC interactions compared to **1**/DMPC interactions are also apparent in the molecular areas extracted at 25 mN/m (Figure 4B, empty squares). The **2**/DMPC monolayers with DMPC mole ratios greater than 0.3 yield molecular areas according to the additivity rule (Figure 4B, empty squares). This result stands in contrast to the **1**/DMPC monolayers for which a slightly positive deviation from the additivity rule was detected (Figure 3B, empty squares).

The BAM images shown in Figure 4C further illustrate the effect of DMPC upon the 2D organization of **2**. The BAM images, recorded at 20 mN/m, demonstrate the pronounced shrinking of the condensed **2** domains as the DMPC mole fraction increases. This phenomenon is consistent with the predominance of the LE phase in the mixed **2**/DMPC films evident in the isothermal analysis (Figure 4A). The segregation and contraction of the condensed domains of **2** might account for the negative deviation from the additivity rule in monolayers displaying high **2**/DMPC mole ratios (Figure 4B, empty squares). Similar to the situation for **1**/DMPC mixture discussed above, a slight variation of the molecular organization with the condensed **2** domains embedded within the fluid DMPC phase might account for the smaller molecular areas recorded (i.e., negative deviation from the additivity rule).

The condensed **2** domains completely disappear at the threshold DMPC mole ratio of 0.4 (BAM data not shown). Indeed, an ostensible threshold of DMPC mole fraction distinguishing between two distinct monolayer configurations is further supported by an examination of the collapse pressures of the monolayers in Figure 4A. The collapse pressures for the **2**/DMPC monolayers up to 0.3 DMPC mole fraction appear to be constant at 45 mN/m, reflecting the collapse of the condensed **2** domains. In contrast, in monolayers containing higher concentrations of DMPC the collapse pressures are lower by 3−5 mN/m and are further modulated according to the ratio between the DMPC and **2**. This observation is ascribed to the formation of an LE phase in which the two molecules are miscible, resulting in a collapse pressure determined according to the mole ratio in the monolayer.

Figure 5 depicts an air/water interface analysis of **3**/DMPC mixtures. A dramatic effect is apparent when DMPC is added to mixed monolayers. The addition of as little as 10% DMPC to a monolayer of **3** significantly alters the film properties: whereas the monolayer of pure **3** exhibits an LC phase beginning in the initial compression all the way to the final collapse (Figure 2C, above), **3**/DMPC (9:1 mol ratio) exhibits a pronounced initial

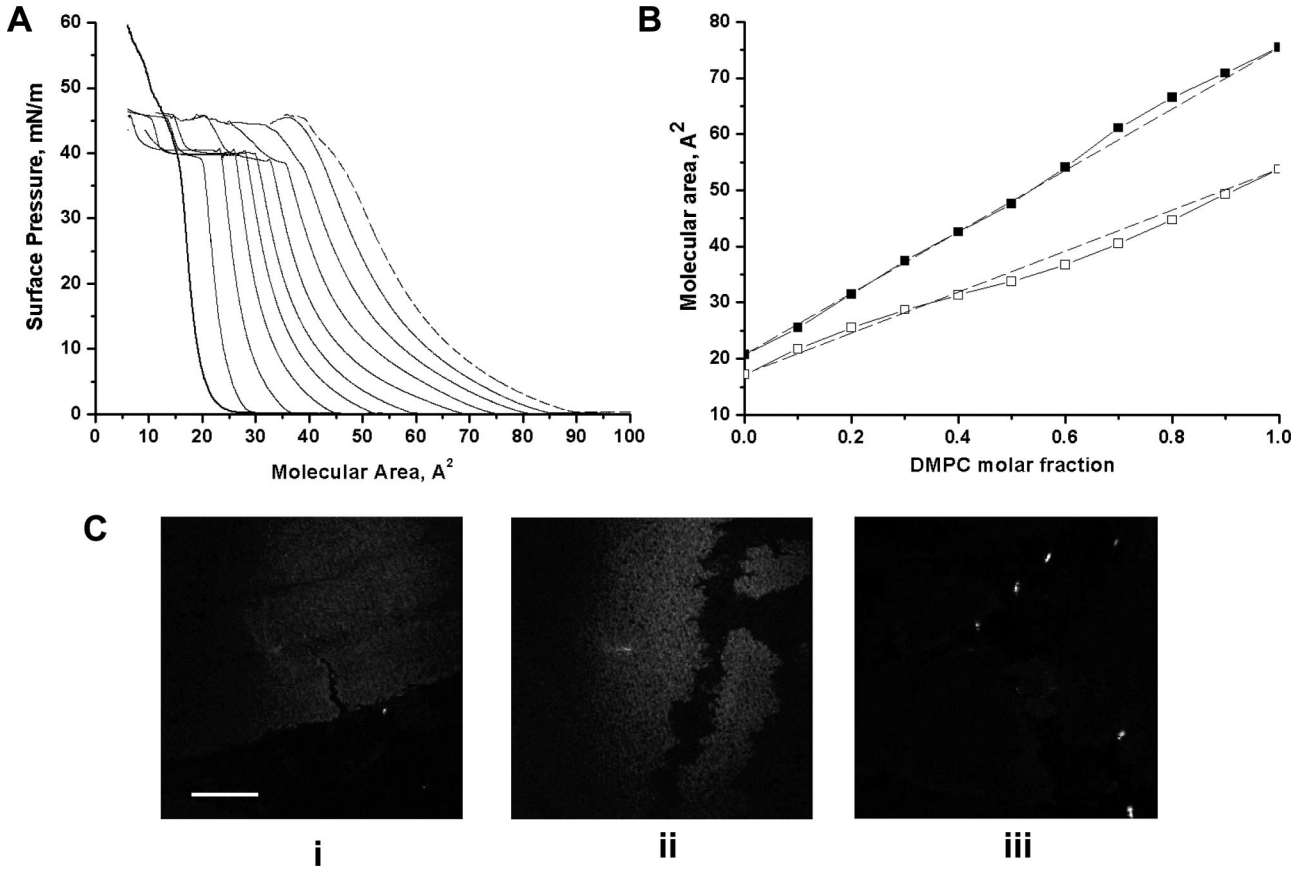

Figure 6. Mixed monolayers of **4** and DMPC. (A) $\pi-A$ isotherms of monolayers having different **1**/DMPC ratios; the solid curve on the left is pure **4**, and the broken curve on the right is pure DMPC. Consecutive curves from left to right contain higher DMPC concentrations increasing in 10% increments (i.e., 9:1, 8:2, 7:3, etc.). (B) Additivity rule diagram; broken lines correspond to mean molecular areas predicted for ideal mixtures (noninteracting species) of **4** and DMPC. Filled squares represent experimental data obtained at 5 mN/m; empty squares represent experimental data obtained at 25 mN/m. The height of the squares corresponds to the experimental error of the average molecular area (1 Å^2/molecule). (C) BAM images recorded at 10 mN/m for **4**/DMPC monolayers: (i) 9:1 mol ratio (**4**/DMPC), (ii) 4:1 mol ratio, (iii) 7:3 mol ratio. The bar corresponds to 100 μm.

LE phase up to an LE−LC transition at around 6 mN/m (Figure 5A, second isotherm from the left), which did not exist in the isotherm of pure **3**. The surface pressure in which the LE−LC transition occurred appeared to be correlated to the mole ratio of DMPC in the mixed monolayers. This is expected because DMPC stabilizes the LE phase of the monolayer; indeed, a sole fluid phase was apparent in the monolayers having a DMPC mole ratio of 0.7 or higher (three isotherms on the right in Figure 5A).

The additivity rule diagram in Figure 5B reflects the interactions between **3** and DMPC. In particular, the formation of a fluid monolayer when DMPC is added to **3** is manifested in the substantial divergence from the broken line of the molecular areas extracted at 5 mN/m (Figure 5B, filled squares). Note, however, that all molecular area values corresponding to the mixed **3**/DMPC monolayers at 5 mN/m (Figure 5B, filled squares), essentially tracing a straight line (shown as a dotted line in Figure 5B), suggesting insignificant molecular interactions between the two components in the fluid phase.

The mean molecular areas of the **3**/DMPC monolayers calculated at 25 mN/m (Figure 5B, empty squares) point to negative deviations from the additivity rule up to a 1:1 (**3**/DMPC) ratio. Such deviations are similar to the results obtained for **2**/DMPC monolayers at high surface pressure (Figure 4B discussed above) and again probably reflect different organization within the condensed domains of **3**, as revealed in the BAM images in Figure 5C. Indeed, the BAM data demonstrate that the condensed "spheres" of **3** are becoming smaller and significantly more abundant as relatively more DMPC molecules are incorporated into the monolayers (Figure 5C).

Figure 6 presents the thermodynamic and microscopic analysis of **4**/DMPC monolayers at the air/water interface. The inclusion of DMPC did not appear to alter the predominant LC phase of **4** at the air/water interface, up to very high concentrations of the phospholipid (Figure 6A). Intriguingly, even though the addition of DMPC did not affect the condensed phase of **4**, the phospholipids induced pronounced film collapse at 40 mN/m. This transition has hardly been detected in the monolayer of pure **4** (left isotherm in Figure 6A). The collapse pressure of **4** at 40 mN/m barely changed upon varying the **4**/DMPC ratio (Figure 6A), indicating that the two molecular constituents are immiscible in the mixed films. This interpretation is supported by the appearance of an additional collapse in the isotherms of the mixed monolayers at around 45 mN/m, ascribed to DMPC (Figure 6A).

The additivity rule analysis (Figure 6B) and BAM data (Figure 6C) lend further support to the apparent segregation between **4** and DMPC in the mixed monolayers. Specifically, the mean molecular areas calculated for the monolayers at different compositions appear to be very close to the broken lines at the two surface pressures, corresponding to ideal mixtures (Figure 6B). The BAM images in Figure 6C similarly show that the mixed films comprise both of the condensed regions of **4** (brighter domains) interfaced with the fluid DMPC monolayer (dark background).

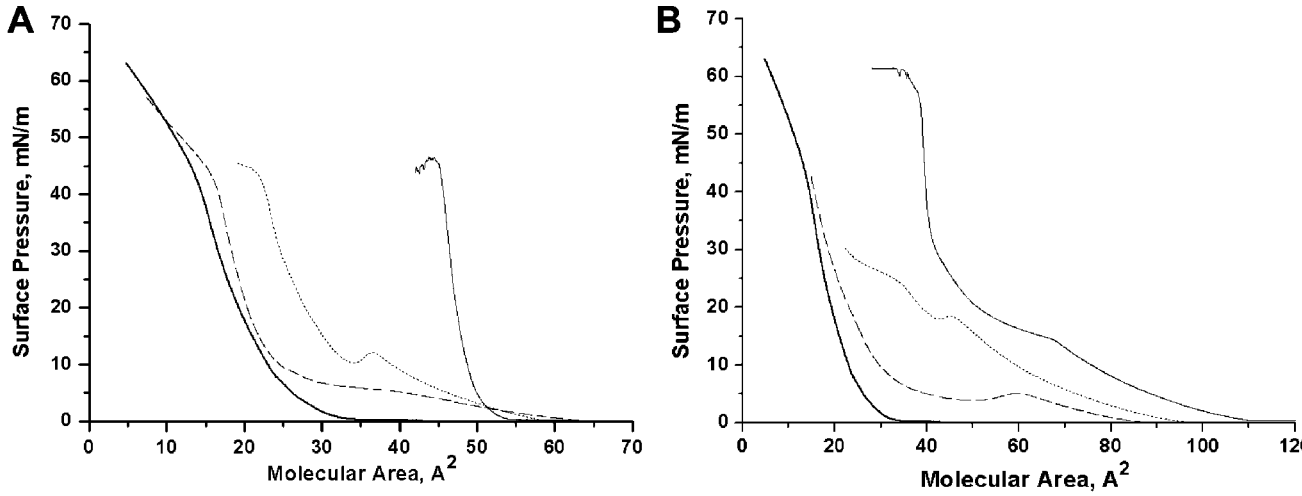

Figure 7. Effects of cholesterol and negative phospholipids. (A) DMPC/cholesterol mixture: pure **3**, solid isotherm on left; DMPC/cholesterol (1:1 mol ratio), solid isotherm on the right; **3**/DMPC/cholesterol (9:0.5:0.5 mol ratio), broken curve; **3**/DMPC/cholesterol (5:2.5:2.5 mol ratio), dotted curve. (B) DMPG: pure **3**, solid isotherm on the left; pure DMPG, solid isotherm on the right; **3**/DMPG (9:1 mol ratio), broken curve; **3**/DMPG (1:1 mol ratio), dotted curve.

DAG-lactone Interactions with Cholesterol and with Negative Phospholipids. Whereas Figures 3−6 examine the effects of DMPC, which is a zwitterionic phospholipid present in physiological membranes, upon the organization and thermodynamic properties of the DAG lactone derivatives we further investigated the contribution of other membrane constituents having different structural and electronic properties, including cholesterol[27] and negatively charged dimyristoylphosphatidylglycerol (DMPG)[28] (Figure 7). Figure 7 presents the $\pi-A$ isotherms of **3** mixed with DMPC/cholesterol (Figure 7A) and in mixed monolayers with DMPG (Figure 7B). Importantly, although Figure 7 summarizes the interactions of cholesterol and DMPG with **3**, qualitatively similar results were obtained for the other DAG-lactones studied (data not shown).

Figure 7A depicts the results of the isothermal compression of **3** mixed with DMPC/cholesterol solutions at equimolar concentrations of the lipids. The DMPC/cholesterol monolayer (1:1 mol ratio) adopts a uniformly liquid-condensed phase,[29] giving rise to the steep $\pi-A$ isotherm shown in Figure 7A (solid isotherm on the right). The effect of incorporating **3** within the monolayer, however, is dramatic. The isotherm of **3**/DMPC/cholesterol (5:2.5:2.5 mol ratio, dotted curve in Figure 7A) features a pronounced liquid-expanded phase over a significant molecular area range. Importantly, the shape of the isotherm is almost identical to the one obtained for **3**/DMPC (no cholesterol) at a 7:3 mol ratio as depicted in Figure 5A (fourth isotherm from the left).

Furthermore, the isotherm of **3**/DMPC/cholesterol (9:0.5:0.5) in Figure 7A (broken curve) has a very strong resemblance to the **3**/DMPC (9:1) isotherm in Figure 5A (second isotherm from the left). The monolayer compression results for both mixtures of **3**/DMPC/cholesterol suggest that DAG-lactone exhibits a much more pronounced interaction with DMPC than with cholesterol. Indeed, the isotherm of **3**/DMPC/cholesterol (9:0.5:0.5) (broken line, Figure 7A) highlights the striking fluidization effect of incorporating just 5% DMPC into the film, transforming the LC phase observed either in the case of **3** by itself (solid curve in Figure 7A, left) or in the DMPC/cholesterol monolayer (solid curve in Figure 7A, right) into a new LE phase of the **3**/DMPC/cholesterol mixture.

$\pi-A$ isotherms recorded for **3**/DMPG monolayers are depicted in Figure 7B. DMPG exhibits an LE−LC phase transition at 1 6mN/m, which is significantly modified when **3** is further incorporated into the monolayers (both broken and dotted isotherms in Figure 7B). The shapes of the isotherms at the two **3**/DMPG molecular ratios examined (dotted and broken curves in Figure 7B) match to a very high degree the corresponding compression data of the **3**/DMPC monolayers (depicted in Figure 5A), indicating that the phospholipid headgroups probably do not play a significant role in the interactions with the DAG-lactones.

Discussion

The surface-pressure/area isotherms and BAM data in Figures 1−6 illuminate the self-assembly properties and lipid interactions of DAG-lactone derivatives displaying different side residues. Overall, the experimental data underscore two main conclusions. First, the side groups R of the DAG-lactones examined (Figure 2) intimately affected the assembly properties and lipid interactions of the molecules, and second, lipid interactions play a significant role in the monolayer organization of the molecules.

The $\pi-A$ isotherms in Figure 2 point to clear correlations between the molecular properties of the DAG-lactones, particularly the contribution of R and the organization at the air/water interface. Thus, the conjugated π systems extending to side chain R in **3** and **4** result in strong π-stacking interactions leading to characteristic condensed-phase behavior throughout the entire surface-pressure range of the compression isotherms (Figure 2C,D). In contrast, the R residues in **1** and **2** contribute minimally to interactions with adjacent molecules, resulting in LE phases of both DAG-lactones at low surface pressures (Figure 2A,B). **1**, for example, exhibits the most pronounced liquid-expanded phase, extending over molecular areas of more than 30 Å^2 (Figure 2A). This result is ascribed to the presence of the hydrogen as R. In comparison, **2**, in which R constitutes the

(26) Gaines, G. L., Jr. *Insoluble Monolayers at Liquid-Gas Interfaces*; Wiley-Interscience: New York, 1966.

(27) Alberts, B.; Johnson, A.; Lewis, J.; Raff, M.; Roberts, K.; Walter, P. *Molecular Biology of the Cell*, 4th ed.; Garland Science: New York, 2002; p 588.

(28) Prenner, E. J.; Lewis, R. N. A. H.; Kondejewski, L. H.; Hodges, R. S.; McElhaney, R. N.; *BBA: Biomembranes* 1999, *1417*, 211–223. Differential scanning calorimetric study of the effect of the antimicrobial peptide gramicidin S on the thermotropic phase behavior of phosphatidylcholine, phosphatidylethanolamine and phosphatidylglycerol lipid bilayer membranes.

(29) Hirshfeld, C. L.; Seul, M.; *J. Phys. (Paris)* 1990, *51*, 1537–1552. Critical mixing in monomolecular films: pressure-composition phase diagram of a two-dimentional binary mixture

bulkier methoxy residue, adopts a more compact monolayer and a less-pronounced LE phase (Figure 2B), corresponding to the higher affinity between the molecules at the air/water interface.

Experiments examining binary monolayers of DAG-lactones and DMPC (Figures 3−6) reveal an interesting interplay between the two constituents. In particular, R appears to be intimately involved in the interactions of the DAG-lactones with the phospholipid molecules. A pronounced effect of DMPC, which is specifically apparent for DAG-lactones **2** and **3**, was the predominance of the LE phase within the mixed monolayers. Thus, the LE−LC transition of **2** and **3** (Figures 4A and 5A, respectively) appeared at progressively higher surface pressures as the ratio between DMPC and the DAG-lactones increased.

The direct relationship between phospholipid concentration and LE−LC surface pressure is an indication of the miscibility of the two components. An elucidation of the extent of miscibility within mixed films is aided by the application of the Crisp phase rule,[30] applied in this work for the analysis of the relationship between the surface pressure and the molecular area at the phase transitions. Specifically, for a two-component monolayer, the Crisp rule determines that the number of degrees of freedom at the interface between the two molecular species corresponds to $F = 3 - q$, where q is the number of surface phases at equilibrium with each other.[22,31] This simple equation essentially indicates that when the two components are miscible only two uniform phases will be present in equilibrium at a phase transition (i.e., $q = 2$). Thus, in this situation the system would possess one degree of freedom, implying a first-order relation between the transition pressure and film composition. Conversely, if the two components are immiscible, then three surface phases will coexist at a phase transition (of one of the components) and accordingly zero degrees of freedom. This will result, for example, in constant surface pressure during the phase transition in such films.

The application of the phase rule provides insight into the extent of miscibility of the DAG-lactones and DMPC. For **2** and **3**, increasing the DMPC mole ratio destabilizes the condensed phase of the DAG-lactone, causing a gradual increase in the surface pressure of the phase transition until the LC phases completely disappear when the DMPC concentration in the monolayer approaches 40% (Figures 4A and 5A). Accordingly, these data indicate a dependence of the LE−LC phase transition upon film composition (i.e., one degree of freedom) and thus miscibility within the mixed monolayers. In contrast, the constant collapse pressure at around 40 mN/m observed in **4**/DMPC monolayers with different mole ratios (Figure 6A) points to the immiscibility of the two molecular species (zero degrees of freedom).

The data clearly indicate that the stronger the self-assembly of the DAG-lactones at the air/water interface the weaker the dissolution effect that DMPC exerts upon the condensed phases of the molecules toward the formation of a liquid-expanded monolayer. A particularly intriguing result in that regard concerns the mixed **3**/DMPC monolayers (Figure 5). In that system, the incorporation of as little as 10% DMPC into a monolayer of **3** significantly altered the film properties, transforming the monolayer into a highly fluidic film.

A comparison of the experimentally determined mean molecular areas with the values predicted from the additivity rule provides another powerful tool for evaluating the interactions of the DAG-lactones with DMPC. The absence of significant interactions was generally observed either in the complete LE phases of the mixed monolayers or in situations in which the condensed phase of the DAG-lactone derivative was segregated from DMPC (particularly in the **4**/DMPC monolayers). Negative deviations from the additivity rule were observed, however, in films exhibiting higher DAG-lactone/DMPC ratios, indicating that the condensed domains of the DAG-lactones in such films were organized slightly differently as compared to the pure compounds. Interestingly, repulsion between the DAG-lactones and the DMPC molecules was also detected for **1** (at high surface pressure) and for **2** (at low pressure), respectively, leading to positive deviations from the additivity rule. Overall, the additivity rule analyses demonstrate that mutual effects exist between the DAG-lactones and DMPC and, furthermore, that interactions between the two constituents were significantly modulated by R.

Additional experiments probed the contributions of cholesterol and negatively charged phospholipids, respectively, upon the interactions and surface organizations of the DAG-lactones (Figure 7). Data obtained for **3** demonstrated a clear preference of the DAG-lactone to adopt a fluid phase with DMPC rather than incorporating into the condensed phase of cholesterol (Figure 7A). This result might be biologically significant because cholesterol is known to form condensed lipid domains (sometime referred to as "lipid rafts") in physiological membranes.[32] Ligands excluded from such domains might therefore selectively regulate PKC responses that do not involve lipid raft signaling complexes.

The comparison between the compression profiles of **3** with DMPC and DMPG (Figure 7B) showed that the assembly properties of the DAG-lactone do not depend upon the type and charge of the phospholipid headgroup. These results also suggest that the fluidity of the lipid phase is a primary factor affecting the membrane association of DAG lactones. Finally, it should be borne in mind that the actual concentrations of the DAG-lactones under typical biological conditions correspond to appreciably lower DAG-lactone/phospholipid ratios than those applied in this study, so the principles emerging from the current studies need to be extrapolated to predict the biological behavior in actual membranes.

Acknowledgment. This research was supported in part by the Intramural Research Program of the NIH, National Cancer Institute, Center for Cancer Research.

Supporting Information Available: Synthesis methods. This material is available free of charge via the Internet at http://pubs.acs.org.

LA802204N

(30) Crisp, D. J. *Surface Chemistry Suppl. Research* Butterworths: London, 1949; pp 17−23.

(31) Birdi, K. S. *Self-Assembly Monolayer Structures of Lipids and Macromolecules at Interfaces*; Kluwer Academics/Plenum Publishers: New York, 1999.

(32) Simons, K.; Ikonen, E.; *Nature* 1997, *387*, 569–572. Functional rafts in cell membranes.